Japanese Journal of Applied Physics
Vol. 47, No. 9, 2008, pp. 7216–7219



# Luminescence Properties of Amorphous Carbon Films Formed Using Supermagnetron Plasma

Katsutoshi SAKURAI, Haruhisa KINOSHITA*, Genji OHNO, Yoichiro NAKANISHI, and Masaya KUBOTA

*Research Institute of Electronics, Shizuoka University, 3-5-1 Johoku, Naka-ku, Hamamatsu 432-8011, Japan*

(Received February 25, 2008; accepted May 3, 2008; published online September 12, 2008)

Polymer-like amorphous carbon (a-$CO_x$:H and a-$CN_x$:H) films were deposited using two types of supermagnetron plasma, i.e., Ar sputter and i-$C_4H_{10}/N_2$ chemical vapor deposition (CVD), respectively. The $sp^2$ clustering of these films was proved experimentally by Raman scattering and the estimation of optical band gap. The photoluminescence (PL) and electroluminescence (EL) properties of these films were measured and analyzed. As a result, a-$CO_x$:H films deposited by Ar sputtering showed similar peak energies for PL and EL (1.9–2.0 eV), while a-$CN_x$:H films deposited by i-$C_4H_{10}/N_2$ CVD showed large shifts between peak energies for PL (2.2 eV) and EL (1.7 eV). The differences in peak energies in the latter were ascribed to the luminescence characteristics caused by $sp^2$ clusters embedded in the $sp^3$ carbon matrix.
[DOI: 10.1143/JJAP.47.7216]

KEYWORDS: polymer-like amorphous carbon, photoluminescence (PL), electroluminescence (EL), Raman scattering, supermagnetron plasma, chemical vapor deposition (CVD), sputter

## 1. Introduction

Hydrogenated amorphous carbon (a-C:H) films have attracted much interest because of their many unique properties suited to many kinds of optoelectronic and vacuum microelectronic devices, such as light emission diodes and field electron emission devices.[1] Polymer-like amorphous carbon seems to be a promising material as an active layer in electroluminescent devices and light-emitting diodes. These films are formed by various deposition methods such as electron cyclotron resonance (ECR) plasma chemical vapor deposition (CVD),[2] pulsed filtered vacuum arc deposition,[3] magnetron sputtering,[4] plasma CVD,[5] and supermagnetron plasma CVD.[6] Because of these many deposition methods, the formed polymer-like amorphous carbon films have various properties. It is rather difficult to form films with similar properties using different deposition methods. Polymer-like hydrogenated amorphous carbon nitride (a-$CN_x$:H) deposited by supermagnetron plasma CVD was investigated by Kinoshita *et al.*[6] Using supermagnetron plasma CVD, photoluminescences (PLs) with various peak energies were observed in the deposited a-$CN_x$:H films. The peak energy was decreased by increasing the upper electrode rf power (UPRF) of the supermagnetron plasma apparatus. In spite of the relatively bright PL performance of a-$CN_x$:H films, the luminescence mechanism is hardly known, as it is caused by complex CC bond structures. To analyze the luminescence mechanism, it is very effective to observe the electroluminescence (EL) of polymer-like amorphous carbon films. EL properties have been investigated by several groups;[7–9] however, it has not been easy to determine the EL mechanism, and reports on EL itself are limited.

In this study, we report the room-temperature properties of PL and EL of two kinds of amorphous carbon films formed using plasma sputter deposition (SD) and plasma CVD.

## 2. Experimental Procedure

Polymer-like hydrogenated amorphous carbon oxide (a-$CO_x$:H) SD and a-$CN_x$:H CVD films were deposited using a supermagnetron plasma deposition apparatus.[6] The experimental arrangements used for the deposition of (a) a-$CO_x$:H SD and (b) a-$CN_x$:H CVD films are shown in Figs. 1(a) and 1(b), respectively. In each apparatus, two independent rf power sources with the same rf frequency (13.56 MHz) were supplied to two electrodes with respect to the grounded metal chamber. The upper electrode was covered with a graphite plate. The phase difference between the two rf voltages was controlled at about 180°, at which the plasma density became higher than that of conventional magnetron plasma.[10] The deposition substrates were placed on the lower electrode. The lower electrodes were heated to 30 °C in SD and CVD.

In the deposition of a-$CO_x$:H SD films, a magnetic field of about 140 G was applied parallel to each electrode surface. At the upper and lower electrode rf powers (UPRF/LORF) of 100 W/ground (GND), a graphite target and Ar gas (60 sccm for 13–20 Pa, and 100 sccm for 27 Pa) were used for the plasma SD of a-$CO_x$:H, whose oxygen and hydrogen atoms were incorporated from the water vapor residue inside the chamber.

In the deposition of a-$CN_x$:H CVD films, a magnetic field of about 80 G was applied parallel to each electrode surface. At the UPRF/LORF of 5/5 W, i-$C_4H_{10}/N_2$ mixed gas (50/120 sccm) at 4 Pa was used for the deposition of a-$CN_x$:H films. In the CVD apparatus shown in Fig. 1(b), a load-lock chamber is installed to prevent the contamination of the plasma process chamber by air. Therefore, the amount of water vapor residue inside the plasma process chamber is less than that in the SD apparatus shown in Fig. 1(a).

Oxygen and nitrogen atom concentrations were measured using X-ray fluorescence spectroscopy (XFS). The bonding configurations of these films were measured using a Fourier transform infrared (FTIR) spectrometer. Raman measurement was carried out on a Raman apparatus using the 532 nm line of an yttrium aluminum garnet second harmonic generation (YAGSHG) laser. We present the Raman spectra recorded in the wave number range of 1167–1820 $cm^{-1}$. The PL was measured at room temperature using He–Cd laser (3.82 eV) excitation. Optical band gap ($E_G$) was estimated from the Tauc plot on the basis of the relation $(\alpha h\nu)^{1/2} = A(h\nu - E_G)$, where $A$ is a constant and $h\nu$ is the

*E-mail address: rdhkino@ipc.shizuoka.ac.jp

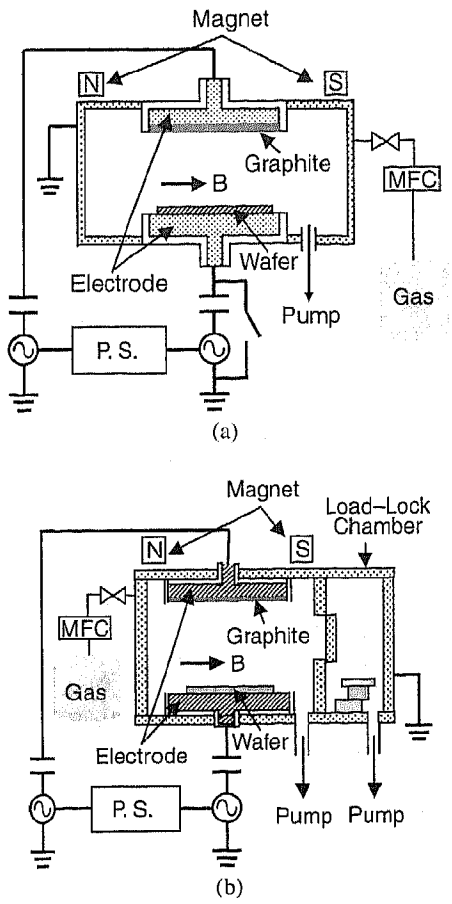


Fig. 1. Schematics of supermagnetron plasma deposition apparatuses used for formation of (a) a-$CO_x$:H SD and (b) a-$CN_x$:H CVD.

photon energy,[11] using the optical absorption data obtained using an ultra violet/visible/near infrared (UV/vis/NIR) spectrometer.

Two types of EL devices (EL1 and EL2) were fabricated using a-$CO_x$:H and a-$CN_x$:H films. EL1 [indium tin oxide (ITO)/a-$CO_x$:H/LiF/Al] has four layers: ITO as the transparent anode layer, a-$CO_x$:H film as the active layer, LiF as the electron-injection layer, and Al as the cathode layer. EL2 [ITO/*N*,*N*′-di(naphthalene-1-yl)-*N*,*N*′-diphenyl-benzidine ($\alpha$-NPD)/a-$CN_x$:H/tris(8-hydroxyquinolinato)aluminum ($Alq_3$)/LiF/Al/Au] has four layers: ITO as the transparent anode layer, $\alpha$-NPD as the hole transport layer, a-$CN_x$:H film as the active layer, $Alq_3$ as the electron transport layer, LiF as the electron injection layer, and Al/Au as the cathode layer. The $\alpha$-NPD, $Alq_3$, LiF layers, and Al cathode were deposited by the vacuum evaporation method, and the Au cathode was deposited by the sputtering method. The EL spectra of these devices were measured with a multichannel spectrophotometer.

## 3. Results and Discussion

In the case of SD films deposited on Si wafers, the gas pressure dependences of deposition rate and optical band gap are shown in Fig. 2. Deposition rate decreased from 2.2 to 1.1 nm/min with an increase in gas pressure from 13 to 27 Pa. This decrease in deposition rate might have been caused by a decrease in $Ar^+$ ion energy (in proportion to the direct current self-bias voltage of the upper electrode) with

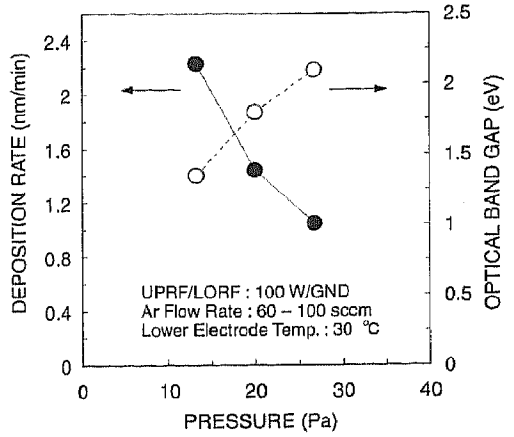


Fig. 2. Gas pressure dependences of deposition rate and optical band gap of SD (a-$CO_x$:H, Ar, 100 W/GND) film.

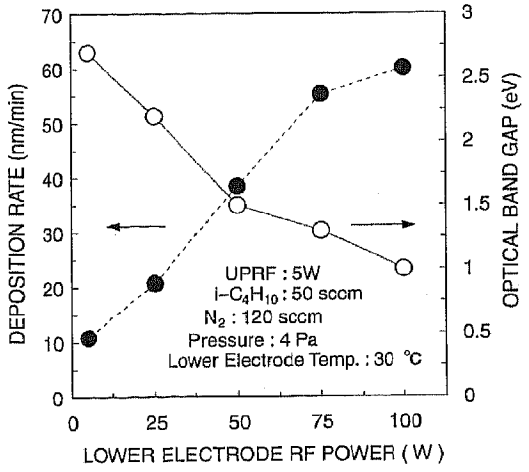


Fig. 3. LORF dependences of deposition rate and optical band gap of CVD (a-$CN_x$:H, i-$C_4H_{10}$/$N_2$, 5 W UPRF) film.

an increase in gas pressure. With a decrease in $Ar^+$ sputtering energy, the sputter rate of the graphite target decreased. Optical band gap increased from 1.4 to 2.1 eV with an increase in gas pressure from 13 to 27 Pa. This increase in optical band gap was caused by the decrease in the $sp^2$ cluster size inside the $sp^3$ matrix.[12]

In the case of CVD films deposited on Si wafers at an UPRF of 5 W, the LORF dependences of deposition rate and optical band gap are shown in Fig. 3. Deposition rate was increased from 11 to 60 nm/min with an increase in LORF from 5 to 100 W. This increase in deposition rate was caused by an increase in plasma density. Optical band gap decreased from 2.7 to 1.0 eV with an increase in LORF from 5 to 100 W. This decrease in optical band gap might have been caused by an increase in the $sp^2$ cluster size in the $sp^3$ matrix and a decrease in $\pi$–$\pi^*$ gap.

The FT-IR absorption spectra of SD and CVD films were measured, and are shown in Fig. 4. An SD film was deposited at 100 W/GND and an Ar gas pressure of 27 Pa, and a CVD film was deposited at 5/5 W and i-$C_4H_{10}$/$N_2$ gas pressure of 4 Pa. An absorption band at 2930 $cm^{-1}$ ($CH_3$, $CH_2$, and CH bonds)[6] was observed in both SD and CVD films. A broad absorption band at 3200–3700 $cm^{-1}$ (OH bonds)[13] was observed in the SD film, but not in the CVD film.

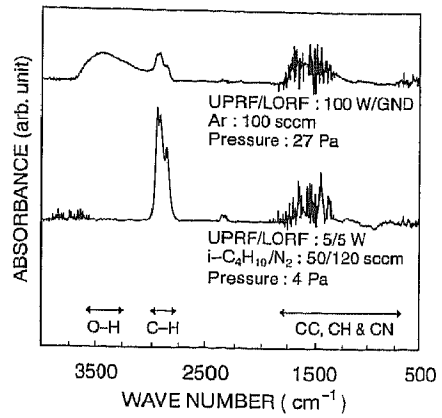


Fig. 4. FT-IR absorption spectra of SD (100 W/GND) and CVD (5/5 W) films.

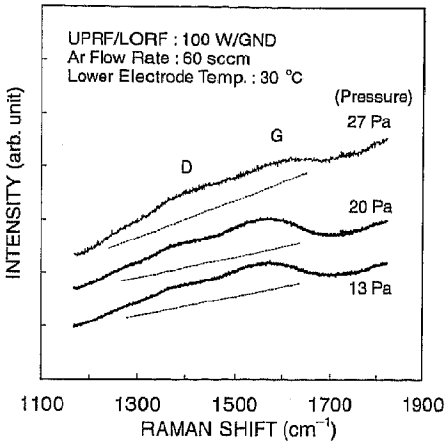


Fig. 5. Raman spectra of SD (a-$CO_x$:H, Ar, 100 W/GND) films deposited at Ar gas pressures of 13, 20, and 27 Pa.

The N and O atom concentrations of the SD (a-$CO_x$:H; 100 W/GND) and CVD (a-$CN_x$:H; 5/5 W) films were measured using XFS, and found to be 0 (N) and 19 mass % (O) for the SD film and 4 (N) and 4 mass % (O) for the CVD film, respectively. In the case of the CVD (a-$CN_x$:H; 5/5 W) film, no broad absorption band at 3200–3700 $cm^{-1}$ (OH bonds in C–OH structure) was observed. Therefore, $H_2O$ molecules were estimated to be absorbed in the voids of the a-$CN_x$:H films after exposure to the atmosphere.

Raman spectra excited by a 532 nm line for the SD (a-$CO_x$:H; 100 W/GND) films of different deposition gas pressures are shown in Fig. 5. The spectra indicate the characteristics of amorphous carbon because of the presence of the G and D bands, which appeared at 1560 and 1380 $cm^{-1}$, respectively. The G band belongs to the stretching mode of rings and chains, which contain $sp^2$-hybridized carbon atoms, while the D band corresponds to the breathing mode of these rings.[14,15] The Raman spectra of three films (13, 20, and 27 Pa) were observed together with broad luminescence spectra. As is clearly seen in Fig. 5, in the film deposited at a gas pressure of 27 Pa, the Raman scattering intensity in the D band region ($I_D$) (peak at about 1380 $cm^{-1}$) is greater than that in the G band region ($I_G$) (peak at about 1560 $cm^{-1}$). Moreover the luminescence intensity of the film deposited at 27 Pa is greater than those of other films (13 and 20 Pa). In the 27 Pa film, the optical band gap

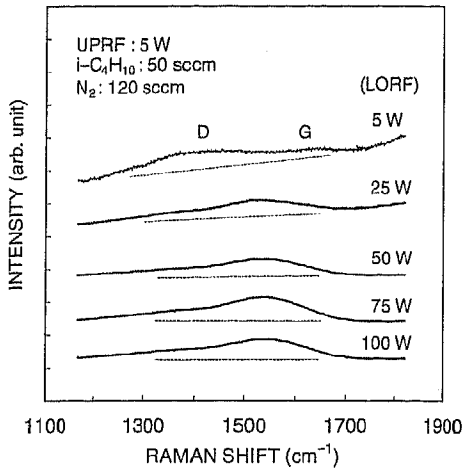


Fig. 6. Raman spectra of CVD (a-$CN_x$:H, i-$C_4H_{10}/N_2$, 5 W UPRF) films deposited at LORFs of 5, 25, 50, 75, and 100 W.

is greater than those of other films (13 and 20 Pa), and $I_D$ is greater than $I_G$. Therefore, the degree of $sp^2$ clustering decreased and the size of $sp^2$ clusters decreased as gas pressure was increased from 13 to 27 Pa.[15]

The Raman spectra of the CVD (a-$CN_x$:H; gas pressure of 4 Pa) films of different LORFs are shown in Fig. 6. The Raman spectra of two films (LORFs of 5 and 25 W) were observed together with the broad luminescence spectra. The other three films (50, 75, and 100 W) showed no luminescence. As can be seen in the 5 W film shown in Fig. 6, the D band intensity $I_D$ (peak at about 1400 $cm^{-1}$) is greater than the G band intensity $I_G$ (peak at about 1620 $cm^{-1}$). In the other films (25–100 W), however, $I_D$s are less than $I_G$s. The luminescence intensity of the 25 W film was less than that of the 5 W film; the other film (50–100 W) showed no luminescence. By the Raman scattering experiments (Fig. 6) and optical band gap estimation (Fig. 3), we found that the degree of $sp^2$ clustering and the size of $sp^2$ clusters were decreased when LORF was decreased from 100 to 5 W.[15]

Figure 7 shows the PL and EL spectra of SD film deposited at 100 W/GND and an Ar gas pressure of 27 Pa. The peak wavelengths of the PL and EL spectra were similar (630–650 nm; 1.9–2.0 eV). The PL and EL peak energies (1.9–2.0 eV) of the SD film were slightly less than the optical band gap of the SD film (2.1 eV). The other SD films (13 and 20 Pa) showed weak PLs, and it was not easy to measure their ELs.

The PL and EL spectra of CVD film deposited at 5/5 W and i-$C_4H_{10}/N_2$ gas pressure of 4 Pa are shown in Fig. 8. In the figure, the PL spectrum of $\alpha$-NPD and the EL spectrum of $Alq_3$ are shown as references. Peak wavelengths show a large difference between the PL and EL spectra, at 555 nm (2.2 eV) and 740 nm (1.7 eV), respectively. The PL and EL peak energies of the CVD films (2.2 and 1.7 eV) were less than the optical band gap (2.7 eV). The CVD film deposited at a LORF of 25 W showed a very weak PL, and it was difficult to measure its EL, while the other CVD films (50 and 100 W) showed no PL or EL.

The peak energy shifts of PL and EL for the SD and CVD films shown in Figs. 7 and 8 are important in investigating the luminescence properties of amorphous carbon films. Luminescence occurs by the recombination of an electron

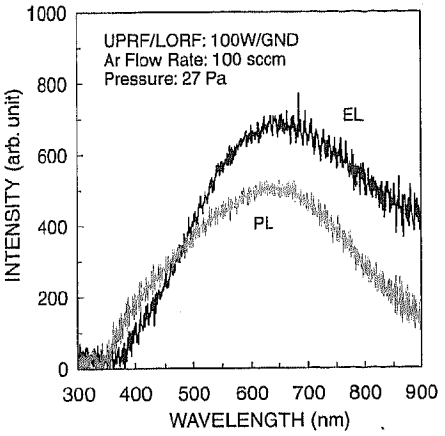


Fig. 7. PL and EL spectra of SD (100 W/GND) film deposited at Ar gas pressure of 27 Pa.

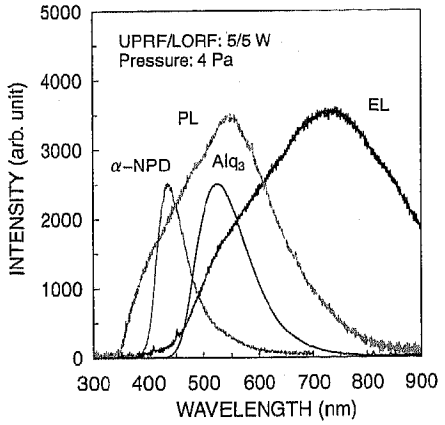


Fig. 8. PL and EL spectra of CVD (5/5 W) film deposited at i-$C_4H_{10}/N_2$ gas pressure of 4 Pa. The PL spectrum of $\alpha$-NPD and the EL spectrum of $Alq_3$ are shown as references.

($\pi^*$ state) and a hole ($\pi$ state) in the $\pi$ orbitals of $sp^2$ sites embedded in the $sp^3$ carbon matrix.[16,17] PL is usually measured under a free electric field while EL is measured under a strong electric field. In the case of a pure organic material such as $\alpha$-NPD, the peak energies of PL and EL are similar.[18] The molecular structure of $\alpha$-NPD is unique; therefore, the luminescence center is simple. As a result, the peak energies of the PL and EL of $\alpha$-NPD became similar. Likewise, in the case of the SD film, the size and structure of the luminescent $sp^2$ cluster are believed to be simple. Therefore, the peak energies of PL and EL became similar. In the case of the CVD film, on the other hand, the size and structure of the luminescent $sp^2$ cluster are believed to be complex, because the CVD film is formed from a hydrocarbon mixed gas of i-$C_4H_{10}/N_2$. This mixed gas would form $sp^2$ clusters with complex structures such as chain and ring structures.[17] These $sp^2$ clusters of various sizes and structures form various kinds of luminescent centers. Under a strong electric field, electrons and holes in the CVD film transport relatively large $sp^2$ clusters by hopping and induce radiative recombination. In the case of the PL of the CVD film, on the other hand, luminescent $sp^2$ clusters are believed to be relatively small. The spatial confinement size of electron hole pairs, i.e., the size of $sp^2$ clusters, determines the energy difference between the $\pi$–$\pi^*$ states due to the quantum size effect.[17] This is hypothesized to be reason, in the case of the CVD film, a large peak energy shift between the PL and EL spectra was observed, as shown in Fig. 8.

## 4. Conclusions

a-$CO_x$:H and a-$CN_x$:H films were formed using supermagnetron plasma Ar SD at 100 W/GND and i-$C_4H_{10}/N_2$ CVD at 4 Pa, respectively. Films with a higher optical band gap, over 2 eV, were deposited at 27 Pa SD (2.1 eV) and 5/5 W CVD (2.7 eV), respectively. The Raman spectra of these films with a relatively high optical band gap showed greater $I_D$ than $I_G$, indicating a decrease in $sp^2$ cluster size with increasing optical band gap.

We fabricated EL devices using SD and CVD films, and the EL and PL luminescence characteristics of these films were compared. The peak energy shift between PL and EL was small for the SD film, but that for the CVD film was large. We found that the large shift in peak energy from 2.2 eV (PL) to 1.7 eV (EL) for the CVD film was ascribed to the difference in the sizes and structures of effective luminescence centers ($sp^2$ clusters) between the PL and EL phenomena. That is, in the PL of the CVD film, electron hole pairs were presumed to be generated in relatively small $sp^2$ clusters in a free electric field, and then recombined with radiating higher-energy photons. In EL (CVD film), electron hole pairs transport relatively large $sp^2$ clusters by hopping in a strong electric field, and then recombine and emit lower-energy photons.

## Acknowledgement

This study was partially supported by a Grant-in-Aid for Exploratory Research, No. 17656014, from the Ministry of Education, Culture, Sports, Science and Technology.

1) H. Kinoshita, M. Yamashita, and T. Yamaguchi: Jpn. J. Appl. Phys. **45** (2006) 8401.
2) T. Schwarz-Selinger, A. von Keudell, and W. Jacob: J. Appl. Phys. **86** (1999) 3988.
3) X. W. Zhang, W. Y. Cheung, N. Ke, and S. P. Wong: J. Appl. Phys. **92** (2002) 1242.
4) M. Clin, O. Durand-Drouhin, A. Zeinert, and J. C. Picot: Diamond Relat. Mater. **8** (1999) 527.
5) S. Kumar, P. N. Dixit, D. Sarangi, and R. Bhattacharyya: J. Appl. Phys. **93** (2003) 6361.
6) H. Kinoshita, R. Ikuta, and K. Sakurai: Thin Solid Films **515** (2007) 4121.
7) M. Zhang, Y. Nakayama, and M. Kume: Solid State Commun. **110** (1999) 679.
8) R. Reyes, C. Legnani, P. M. Ribeiro Pinto, M. Cremona, P. J. G. de Araújo, and C. A. Achete: Appl. Phys. Lett. **82** (2003) 4017.
9) Y. Daigo and N. Matsukura: Diamond Relat. Mater. **13** (2004) 2170.
10) H. Kinoshita, F. Fukushima, M. Kando, Y. Nakagawa, and T. Tsukada: J. Appl. Phys. **88** (2000) 2263.
11) J. Tauc: *Amorphous Liquid Semiconductors* (Plenum Press, New York, 1974) p. 159.
12) A. Ilie, A. C. Ferrari, T. Yagi, S. E. Rodil, J. Robertson, E. Barborini, and P. Milani: J. Appl. Phys. **90** (2001) 2024.
13) D. B. Mawhinney and J. T. Yates, Jr.: Carbon **39** (2001) 1167.
14) J. Schwan, S. Ulrich, V. Vatori, H. Ehrhardt, and S. R. P. Silva: J. Appl. Phys. **80** (1996) 440.
15) A. C. Ferrari and J. Robertson: Phys. Rev. B **61** (2000) 14095.
16) J. Robertson: Diamond Relat. Mater. **5** (1996) 457.
17) M. Füle, J. Budai, S. Tóth, M. Veres, and M. Koós: J. Non-Cryst. Solids **352** (2006) 1340.
18) H. Kajii, T. Tsukagawa, H. Okuno, T. Taneda, K. Yoshino, and Y. Ohmori: Thin Solid Films **393** (2001) 388.